*Desalination and Water Treatment*
www.deswater.com
doi: 10.5004/dwt.2020.26161

202 (2020) 317–326
October

# Removal of triclosan from aqueous solution using thermally treated rice husks

Mutiara Triwiswara[a], Jin-Kyu Kang[b], Joon-Kwan Moon[c], Chang-Gu Lee[d], Seong-Jik Park[e,*]

[a]*Department of Chemical Engineering, Hankyong National University, 327 Jungang-ro, Anseong, Gyeonggi-do, Republic of Korea, email: triwiswara@gmail.com (M. Triwiswara)*
[b]*Environmental Functional Materials and Water Treatment Laboratory, Seoul National University, Seoul 08826, Republic of Korea, email: naengie@gmail.com (J.-K. Kang)*
[c]*Department of Plant Life and Environmental Sciences, Hankyong National University, 327 Jungang-ro, Anseong, Gyeonggi-do, Republic of Korea, email: jkmoon@hknu.ac.kr (J.-K. Moon)*
[d]*Department of Environmental and Safety Engineering, Ajou University, Suwon 16499, Republic of Korea, email: changgu@ajou.ac.kr (C.-G. Lee)*
[e]*Department of Bioresources and Rural System Engineering, Hankyong National University, 327 Jungang-ro, Anseong, Gyeonggi-do, Republic of Korea, Tel. +82-31-670-5131; Fax: +82-31-670-5139; email: parkseongjik@hknu.ac.kr (S.-J. Park)*

Received 14 October 2019; Accepted 22 May 2020

**ABSTRACT**

This study investigated triclosan removal using rice husks thermally treated at 100°C, 300°C, and 500°C. Rice husks were characterized by analyzing their surface morphologies, pore size, pore diameter, specific surface area, elemental composition, and chemical functional groups. The rice husks thermally treated at 300°C (RH-300) displayed higher triclosan removal efficiency than those treated at other temperatures. Adsorption of triclosan onto RH-300 was achieved within 4 h, and the kinetic adsorption data were well described by a pseudo-first-order model. The Langmuir model described the equilibrium adsorption of triclosan to RH-300 more suitably than the Freundlich model did, indicating that triclosan was adsorbed on RH-300 as a monolayer. Positive enthalpy changes and negative free energy change obtained from thermodynamic experiments indicated that triclosan adsorption by RH-300 was endothermic and spontaneous under these experimental conditions. A decrease in triclosan adsorption with an increase in solution pH was more obvious in the RH-300 dosage of 3.33 than 6.67 g/L. As fulvic acid increased from 0–10 mg/L, triclosan adsorption onto RH-300 decreased by 25.3%; changes in triclosan adsorption were not distinct above 10 mg/L. In conclusion, RH-300 is a low-cost and effective material for the removal of triclosan from aqueous solutions.

*Keywords:* Triclosan; Rice husk; Adsorption; Thermal treatment; Pyrolysis

## 1. Introduction

Triclosan is a broad-spectrum anti-microbial agent widely used in health care and veterinary products, such as prescription and non-prescription medications; personal care products, such as toothpaste, soaps, deodorants, cosmetics, and skincare lotions; and other consumer goods [1–3]. Triclosan, a biologically active compound that specifically targets bacteria, can affect the microorganisms in environmental systems [4]. It is also a typical endocrine disruptor that can exert adverse effects on animal organs and affect the reproduction of aquatic organisms, including invertebrates,

* Corresponding author.

fish, amphibians, algae, and plants [4–6]. Potential human health issues related to triclosan include antibiotic resistance, skin irritation, endocrine disruption, and increased prevalence of allergies [7].

For years, triclosan has been percolated into the environment, which raises concerns about its potentially harmful effects on drinking water supplies, ecosystem, and human health [3,6]. In a wastewater treatment plant, up to 90% of triclosan can be removed from incoming flow, but complete removal still cannot be achieved [8]. Therefore, its presence can still be detected in water bodies. In addition, due to its hydrophobicity, triclosan has been detected in soil and sediments, fish tissues, human plasma, breast milk, and urine [8].

In recent years, various techniques have been applied for the removal of triclosan from aqueous media, including direct UV photolysis [9], bioremediation of constructed wetlands [10], biological treatment by microorganisms [11–13], sonoelectrochemical degradation [14], and oxidation [15]. In this context, adsorption has been referenced as an efficient and easy-to-use alternative. Adsorption has fewer processing procedures compared to other methods and produces little sludge [16]. Using this method, environmental pollutants are removed and concentrated on a specific area for better handling and disposal. Materials such as activated carbon and clays [17] have shown a potential pollutant adsorbent capacity due to their high surface area, microporous structure, and a high degree of surface reactivity [16]. However, there is a need to find inexpensive and highly available materials to be used as adsorbents. Agricultural waste is a rich source of adsorbent materials because it is cheap, easy to collect, and environmentally friendly [18].

Several different types of agricultural waste have been used in previous studies as adsorbent material, including jatropha, date pits, groundnut shell, corncob, bamboo, rattan sawdust, oil palm fiber, coconut shell, and coconut husk [19–21]. Rice husk, obtained from rice mills after the separation of rice from paddy, is one of the most widely used agricultural wastes in wastewater treatment. Rice husk is considered suitable for application as an adsorbent material because of its granular structure, insolubility in water, chemical stability, high mechanical strength, and excess availability [22]. Rice husk has been reported to possess the potential to adsorb organic pollutants, including pharmaceutical compounds in aqueous solution [23–25]. In addition, thermal treatment can increase the surface area of the material, thus significantly increasing its adsorbent capacity [24].

Little attention has been paid to the use of rice husks as an adsorbent to remove triclosan. Therefore, this study aimed to investigate the adsorption of triclosan using thermally activated rice husks, which were treated under different temperatures and characterized by analyzing their surface morphologies, pore volume, pore size, specific surface area, elemental composition, and chemical functional groups. We evaluated the triclosan removal efficiency of rice husks thermally treated at different temperatures. The rice husk treatment with the highest triclosan removal efficiency was then used to investigate the adsorption characteristics of triclosan by performing kinetic, equilibrium, and thermodynamic adsorption experiments under batch conditions. In addition, further experiments on the effects of solution pH and fulvic acid on triclosan adsorption were conducted.

## 2. Materials and methods

### 2.1. Chemicals

The triclosan used in this study was supplied by Sigma Aldrich (St. Louis, MO, USA). For the preparation of 1,000 mg/L stock solutions, 100 mg of triclosan was dissolved in 0.1 L of high-performance liquid chromatography (HPLC) grade acetonitrile (Burdick and Jackson, Muskegon, MI, US). To prevent degradation caused by light exposure, the stock solutions were stored under dark conditions at 4°C and used within a month of preparation. Standard solutions were prepared by diluting the stock solutions with 20% acetonitrile (prepared with distilled water) to achieve the desired triclosan concentration. All other chemicals used in this study were purchased from Sigma-Aldrich.

### 2.2. Preparation and characterization of rice husks thermally treated at different temperatures

In this study, the rice husks used were obtained from a local agriculture farm (Anseong, Republic of Korea). The rice husks were washed with plenty of tap water and then rinsed thoroughly using distilled water. This step ensured that all the impurities were removed from the surface of the materials. The clean rice husks were dried in a hot, dry oven for 24 h at 80°C to remove the moisture content. The dried samples were then ground using a ceramic mortar and pestle and sieved to obtain uniform size using No. 30 (0.50 mm) and No. 100 (0.15 mm) U.S. standard sieves. The rice husks were thermally treated in a conventional tube furnace with a horizontal stainless-steel tube (5.5 cm in diameter and 55 cm in length) at different temperatures (100°C, 300°C, and 500°C) for 3 h. Before thermal treatment, $N_2$ gas was injected into the tube furnace to create anoxic conditions. The samples prepared under different conditions were then stored in evaporating dishes for further experiments.

The physical and chemical properties of raw rice husks (RH-NT) and rice husks thermally treated at 100°C, 300°C, and 500°C (RH-100, RH-300, and RH-500, respectively) were investigated using various methods. The surface morphology and chemical composition of the adsorbents were studied using a field-emission scanning electron microscopy (FE-SEM; S-4700, Hitachi, Japan) with an attached energy dispersive spectrometer (EDS). The specimens of the adsorbents were observed at ×1,000 magnification at an accelerating voltage of 15 kV. Before imaging, all samples were coated with gold at 30 mA for 120 s to minimize the charging effect. $N_2$ adsorption–desorption experiments were performed to measure the specific surface area of rice husks using a surface area analyzer (Quadrasorb SI, Quantachrome Instrument, USA). From the $N_2$ adsorption–desorption isotherms, the specific surface area, pore volume, and pore diameter were determined by Brunauer–Emmett–Teller (BET) analysis using a surface area analyzer. Attenuated total reflectance Fourier transform infrared (ATR-FTIR) analysis spectroscopy (Nicolet iS10, Thermo Scientific, USA)

was conducted to identify the chemical functional groups on the surface of the rice husks.

### 2.3. Triclosan adsorption experiments

Triclosan removal by rice husks thermally treated under different temperatures was compared by reacting 0.2 g of each adsorbent with 30 mL of 50 mg/L triclosan solution. The mixtures were then stirred at a speed of 100 rpm at 25°C for 6 h. The speed and temperature of the shaking incubator (SJ-808SF, Sejong Scientific Co., Korea) were maintained constant to ensure that the reacting condition was the same in all the experiments. All batch experiments were performed under these conditions unless otherwise stated. After the reaction, all samples were centrifuged at 4,000 rpm to separate the solution from the rice husks (Combi 514R, Hanil Science Industrial Co., Ltd., South Korea). The residual triclosan concentration in the sample was then quantified using HPLC. All the experiments were conducted in triplicate, and the averages were calculated and used in further analyses. Once the material with the best triclosan removal was found, further batch experiments including kinetic, equilibrium, and thermodynamic experiments and analyses of the influence of pH and fulvic acid on triclosan adsorption were conducted.

Kinetic experiments were performed by varying the reaction time from 0.5 to 6 h with two different initial triclosan concentrations (5 and 50 mg/L). Equilibrium batch experiments were conducted under different initial triclosan concentrations (1–400 mg/L), and samples were analyzed after 6 h of reaction. The thermodynamic adsorption experiments were performed by reacting 0.2 g of rice husk with 30 mL of 50 mg/L triclosan solution for 6 h at reaction temperatures of 15°C, 25°C, and 35°C. The effect of the initial pH on the adsorption of triclosan was evaluated by varying the pH in the range of 4–10 with two different adsorbent dose amounts (3.33 and 6.67 g/L). The original pH of the triclosan solution was 5.6. The pH was adjusted by adding either 0.1 M hydrochloric acid (HCl) or 0.1 M sodium hydroxide (NaOH). The initial and final pH were measured with a pH meter (seven-multi S40; Mettler Toledo, Switzerland). The influence of the presence of fulvic acid on triclosan removal was investigated by varying the fulvic acid concentration from 10 to 100 mg/L. Fulvic acid was purchased from Sigma-Aldrich. The triclosan concentrations and adsorbent dose were fixed to 50 mg/L and 6.7 g/L, respectively.

### 2.4. Chemical analysis

An HPLC system (LC-20AD Shimadzu, Japan) equipped with a Luna C18(2) column (150 mm × 4.6 mm × 5 μm) and a UV-vis detector were used to measure the triclosan concentrations. A detection wavelength of 280 nm [9,26,27] was applied. Acetonitrile/trifluoroacetic acid (0.1%) represented the mobile phase used for the elution and the flow rate was set at 0.8 mL/min through the column. A sample injection volume of 10 μL was used and the column temperature was maintained at 30°C throughout the analyses. For quantification, a calibration plot was performed within the range of experimental concentrations and used when its determination coefficient ($R^2$) was greater than 0.99.

### 2.5. Data analysis

The kinetic data were analyzed using the following pseudo-first-order [Eq. (1)] and pseudo-second-order [Eq. (2)] models:

$$q_t = q_e\left(1 - e^{-k_1 t}\right) \tag{1}$$

$$q_t = \frac{k_2 q_e^2 t}{1 + k_2 q_e t} \tag{2}$$

where $q_t$ is the amount of triclosan removed at time $t$ (mg/L), $q_e$ is the amount of phosphate removed at equilibrium, $k_1$ is the pseudo-first-order rate constant (1/h), and $k_2$ is the pseudo-second-order rate constant (g/L/h). The equilibrium data were analyzed using the following Langmuir [Eq. (3)] and Freundlich [Eq. (4)] isotherm models:

$$q_e = \frac{Q_m K_L C_e}{1 + K_L C_e} \tag{3}$$

$$q_e = K_F C_e^{\frac{1}{n}} \tag{4}$$

where $C_e$ is the concentration of triclosan in the aqueous solution at equilibrium (mg/L), $K_L$ is the Langmuir constant related to the binding energy (L/mg), $Q_m$ is the maximum amount of triclosan removed per unit mass of rice husk (mg/g), $K_F$ is the distribution coefficient ((mg/g)·(L/mg)$^{1/n}$), and $n$ is the Freundlich constant. Values of $K_L$, $Q_m$, $K_F$, and $n$ can be determined by fitting the Langmuir and Freundlich models to obtain the experimental data. All the parameters of the models were estimated by non-linear regression using Sigma-Plot 10.0 with the dynamic fit wizard function.

The thermodynamic properties of the experimental results were analyzed using the following equations:

$$\Delta G^\circ = \Delta H^\circ - T\Delta S^\circ \tag{6}$$

$$\Delta G^\circ = -RT\ln K_e \tag{7}$$

$$\ln K_e = \frac{\Delta S^\circ}{R} - \frac{\Delta H^\circ}{RT} \tag{8}$$

$$K_e = \frac{\alpha q_e}{C_e} \tag{9}$$

where $\Delta G^\circ$ is the change in Gibb's free energy (kJ/mol), $\Delta S^\circ$ is the change in the entropy (J/mol/K), $\Delta H^\circ$ is the change in enthalpy (kJ/mol), $R$ is the gas constant (J/mol/K), $K_e$ is the equilibrium constant between solid and aqueous phases of triclosan (–), and α is the amount of adsorbent (g/L).

## 3. Results and discussion

### 3.1. Characterization of rice husks

The surface morphologies of rice husks thermally treated at different temperatures were investigated using FE-SEM and the resultant images are shown in Fig. 1. Both non-treated and thermally treated rice husks had nodules on their surfaces. As temperatures increased, the valleys between the nodules became deeper. Similar results were observed by Daffalla et al. [28], who reported that pores developed from the decomposition of the raw rice husk structure by heat, converting it to smaller particles with a larger surface area. At 300°C, micro-fragments were observed on the surface of rice husks and these micro-fragments were still present on the surface of rice husks thermally treated at 500°C.

The specific surface area, pore volume, and pore diameter were obtained from a specific surface area analyzer (Table 1). Rice husks without thermal treatment showed both the highest surface area (35.14 $m^2/g$) and the smallest pore diameter (5.11 nm). However, as the thermal temperature increased, smaller specific surface area and bigger pore diameter were obtained, as for RH-100 (24.63 $m^2/g$ and 6.34 nm, respectively) and RH-300 (18.38 $m^2/g$ and 7.56 nm, respectively). This may be due to a higher increase in thermal temperature on rice husks causing an agglomeration effect, diminishing the porosity of rice husks [29]. However, at a calcination temperature of 500°C, there was an increase in specific surface area (29.67 $m^2/g$) and a decrease in pore diameter (6.67 nm). The presence of silica in the ash in an amorphous form could explain this increase in specific surface area of RH-500 [29].

As per the International Union of Pure and Applied Chemistry classification for dimensions of pore size, micropores have pore sizes < 2 nm, mesopores have pore sizes between 2 and 50 nm, and macropores have pore sizes > 50 nm. The BET analysis revealed that the average pore diameter for all the adsorbents fell in the mesopores class, indicating that the adsorbents have a mesoporous nature with a minor presence of micropores [30]. For an adsorbent used in a liquid–solid system, the ability of solutes to access small pores of the adsorbent could be handicapped due to capillary effects. Thus, the adsorbent should possess a well-developed mesoporous texture because mesopores may act as channels leading to micropores [31]. This result indicates that the adsorbents used in this study are suitable for the removal of triclosan in aqueous solution.

The chemical compositions of rice husks thermally treated at different temperatures were obtained from EDS

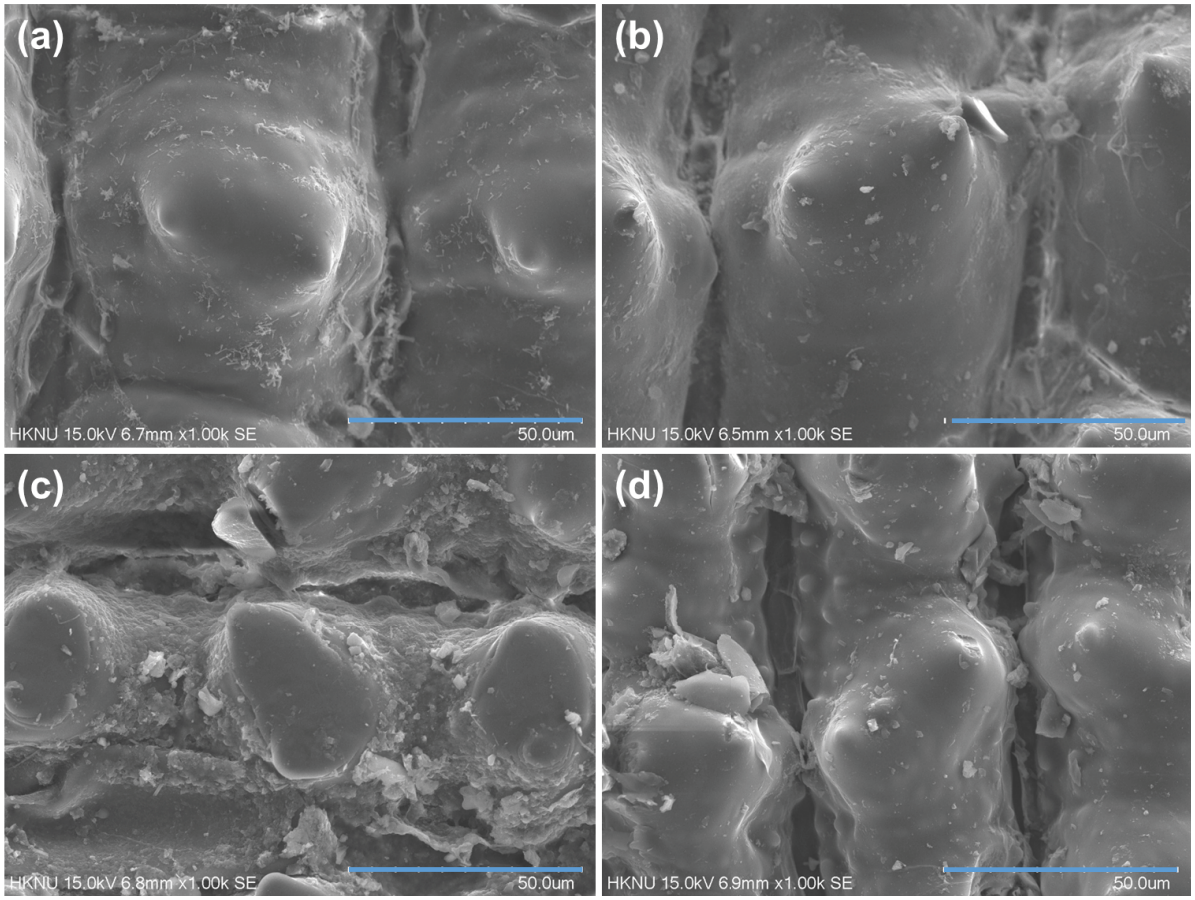


Fig. 1. FE-SEM images of rice husks thermally treated at different temperatures. (a) Untreated rice husks (RH-NT), (b) rice husks thermally treated at 100°C (RH-100), (c) rice husks thermally treated at 300°C (RH-300), and (d) rice husks thermally treated at 500°C (RH-500). The magnification is ×1,000 and scale bar represents 50 μm.

Table 1
Physical properties and chemical composition of rice husks thermally treated under different temperatures.

| Adsorbent | Surface area ($m^2/g$) | Pore volume ($cm^3/g$) | Pore diameter (nm) | Chemical composition (wt %) | | | | |
|---|---|---|---|---|---|---|---|---|
| | | | | C | O | Si | K | Ca |
| RH-NT | 35.14 | 0.04 | 5.11 | 26.2 | 38.9 | 34.6 | 0.2 | 0.2 |
| RH-100 | 24.63 | 0.04 | 6.34 | 27.1 | 35.7 | 36.0 | 0.8 | 0.4 |
| RH-300 | 18.38 | 0.03 | 7.56 | 27.0 | 40.8 | 31.6 | 0.6 | 0.0 |
| RH-500 | 29.67 | 0.05 | 6.67 | 21.3 | 35.2 | 42.6 | 0.9 | 0.0 |

The BET surface area, total pore volume, and average pore diameter were obtained by applying the BET equation at −195.8°C. Chemical compositions were obtained using EDS analysis.

analysis and the results of this analysis are presented in Table 1. The rice husks were mainly composed of C, O, and Si with a small amount of K and Ca. At high temperatures (300°C and 500°C), Ca was diminished from rice husks. As the thermal temperature increased from 100°C to 500°C, the C/O ratio of rice husks decreased from 0.759 to 0.605. The C content of RH-500 was reduced in comparison to other rice husks, but its Si content was the highest. These results are also consistent with the decrease in specific surface area of RH-500 because the thermal treatment generates progressive loss in the carbon phase, while the silicon remains constant.

Fig. 2 compares the evolution of ATR-FTIR spectra for rice husks thermally treated at different temperatures. The wideband ~3,400 $cm^{-1}$, visible for RH-NT and RH-100, can be attributed to –OH stretching vibrations. However, the band at ~3,400 $cm^{-1}$ disappeared in RH-300 and RH-500, which may be due to the disappearance of water molecules from rice husks thermally treated at 300°C and 500°C. Moreover, most samples displayed a similar band with various intensities. The bands at 2,916–2,914; 1,637–1,720; and 779–795 $cm^{-1}$ were assigned to C–H stretching vibrations, C=O stretching vibrations, and C=C bending vibrations, respectively [32–35]. However, as the temperature increased to 500°C, these peaks either disappeared or their intensities were reduced. The bands from double bonds were reduced at higher temperatures. Strong peaks at 1,000–1,100 $cm^{-1}$, assigned to Si–O–Si and Si–O–C bonds, were observed in all rice husks [29]. As the heat treatment temperature increased, the characteristic bands corresponding to organic compounds reduced. However, the peaks corresponding to the Si–O groups were still present in the thermally treated rice husks.

### 3.2. Effect of rice husk thermal treatment on its triclosan adsorption

The effects of thermal treatment on the adsorption potential of rice husks were investigated using non-treated rice husks and rice husks thermally treated at 100°C, 300°C, and 500°C. The results obtained from batch adsorption experiments are shown in Fig. 3. Raw rice husks without thermal treatment adsorbed 5.9 mg/g of triclosan, and this amount increased to 7.3 mg/g when the thermal temperature on rice husks reached 300°C. However, the triclosan removal ability of RH-500 was less than that of RH-300. The effectiveness of triclosan removal by RH-300 could be due to its larger pore size comparative to that of the other rice husks. The increase in pore size provides more access to the inner

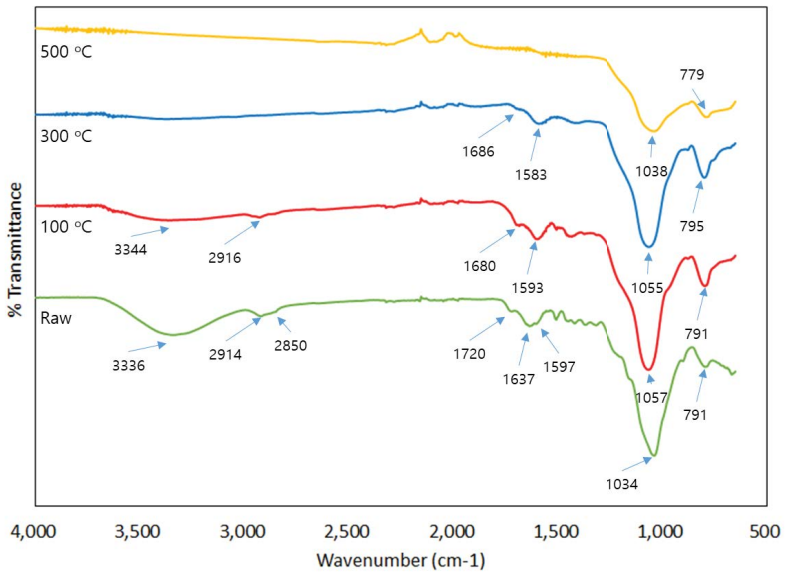


Fig. 2. ATR-FTIR spectrum of rice husks thermally treated at different temperatures (non-treated, 100°C, 300°C, and 500°C).

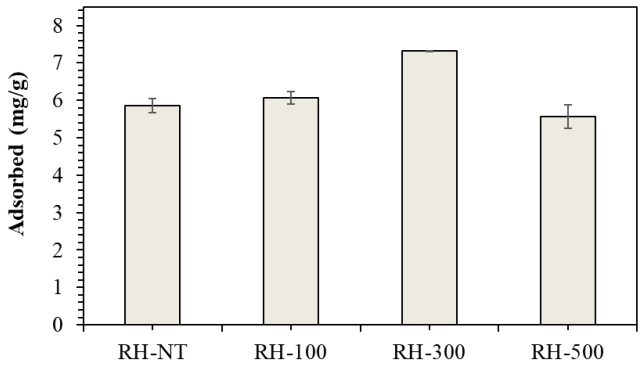


Fig. 3. Effects of thermal temperature (non-treated, 100°C, 300°C, and 500°C) on triclosan adsorbed by rice husks (initial triclosan concentration: 50 mg/L, pH: 5.6, adsorbent dosage: 0.2 g, reaction time: 24 h, agitation speed: 100 rpm, and temperature: 25°C).

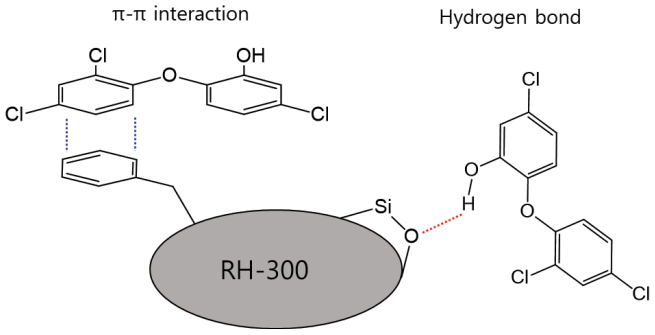


Fig. 4. Schematic diagram depicting the mechanism of adsorption of triclosan onto RH-300.

pores of adsorbents, resulting in higher triclosan removal. The dimensions of triclosan are 1.42 nm × 0.69 nm × 0.75 nm [30], and the micropores are too narrow to allow triclosan to access the pores. Another potential reason for the high triclosan uptake by RH-300 was its chemical characteristics. Its structure still has a carbon–oxygen phase from the organic composition of raw rice husk, and it has phase silicon groups, such as SiOH, available on its surface as a result of the thermal treatment. The presence of all these active groups on the surface favors interaction between triclosan and the adsorbents, resulting in greater efficiency in RH-300 compared to the other treatments [29]. For further experiments, the rice husks thermally treated at 300°C were selected as the adsorbent.

The mechanisms underlying triclosan adsorption on RH-300 can be explained by the hydrophobic effect, electrostatic interaction, hydrogen bonding, and π–π bonds [36]. Triclosan is known to be highly hydrophobic ($\log K_{ow}$ = 4.76) [37] and thus can be adsorbed onto RH-300 via hydrophobic interaction. Triclosan is mainly in its non-ionized form at neutral pH; therefore, electrostatic interaction might not prominently influence the adsorption of triclosan to RH-300 at neutral pH. Cho et al. [37] also proposed triclosan adsorption on carbon nanotubes (CNT) via hydrogen bonding between the OH groups of triclosan and the O-containing groups of CNT. Therefore, it can be inferred that hydrogen bonding occurred between the OH groups of triclosan and the O-containing groups of RH-300, such as –COOH and –O–Si, as shown in Fig. 4. Triclosan can be adsorbed on the surface of rice husks by π–π interaction between the aromatic ring of triclosan and the phenyl group on the surface of RH-300 [36].

### 3.3. Adsorption kinetics

Tests of the adsorption of triclosan by RH-300 at different reaction times were performed at two different initial concentrations (5 and 50 mg/L) of triclosan. As shown in Fig. 5, the adsorption of triclosan reached an equilibrium within 4 h. The data for triclosan adsorption as a function of reaction time were fitted using pseudo-first-order and pseudo-second-order models and the obtained parameters are presented in Table 2. The reaction rates of pseudo-first-order and pseudo-second-order models, $k_1$ and $k_2$, respectively, were slower at higher initial concentrations of triclosan. These results indicate that the adsorption rate decreased as the triclosan concentration increased. As shown in Fig. 5, it took longer to achieve adsorption equilibrium at the higher initial concentrations, implying that adsorption initially occurred on the exterior surface of the adsorbents, followed by the interior surface [38].

The plot of triclosan adsorption as a function of time (Fig. 5) shows that the pseudo-first-order equation agreed well with the data for both concentrations. The determination coefficient ($R^2$) of the pseudo-first-order model was also higher than that of the pseudo-second-order model at both lower and higher initial concentrations. The equilibrium concentrations predicted by the pseudo-first-order model were also closer to the experimental results than those predicted by the pseudo-second-order model. These results indicate that the pseudo-first-order model is more suitable for describing the adsorption of triclosan by RH-300 than the pseudo-second-order model, implying that the rate of adsorption on RH-300 is mainly controlled by diffusion [39].

### 3.4. Adsorption isotherm

The adsorption isotherm of triclosan on RH-300 was studied using fixed amounts of 0.2 g of adsorbent, 30 mL of triclosan solution, and 6 h of contact time. The adsorption isotherm study was performed to investigate how the adsorbate is distributed between the liquid and the solid phases when the adsorption process reaches equilibrium [31]. The adsorbed amount of triclosan onto RH-300 as a function of initial triclosan concentration in the aqueous phase was plotted with model fits of the Langmuir and Freundlich models (Fig. 6). The model parameters obtained from the Langmuir and Freundlich model fits are shown in Table 3. By comparing the determination coefficients ($R^2$) of both models, the higher $R^2$ of the Langmuir model than that of that Freundlich model indicated that the Langmuir model provided a better fit to explain the adsorption of triclosan by RH-300. Based on the results provided, it can be assumed that the surface of RH-300 was homogeneous for triclosan adsorption [18]. The Langmuir model has also

Table 2
Kinetic model parameters obtained from model fitting of the experimental data for adsorption of triclosan by RH-300 at different reaction times

| Initial triclosan concentration (mg/L) | Pseudo-first-order kinetic model parameters | | | Pseudo-second-order kinetic model parameters | | | Observed data |
|---|---|---|---|---|---|---|---|
| | $q_e$ (mg/g) | $k_1$ (1/h) | $R^2$ | $q_e$ (mg/g) | $k_2$ (g/(mg h)) | $R^2$ | $q_e$ (mg/g) |
| 5 | 0.52 | 1.48 | 0.991 | 0.59 | 3.34 | 0.975 | 0.51 |
| 50 | 4.10 | 0.88 | 0.978 | 5.00 | 0.18 | 0.961 | 4.01 |

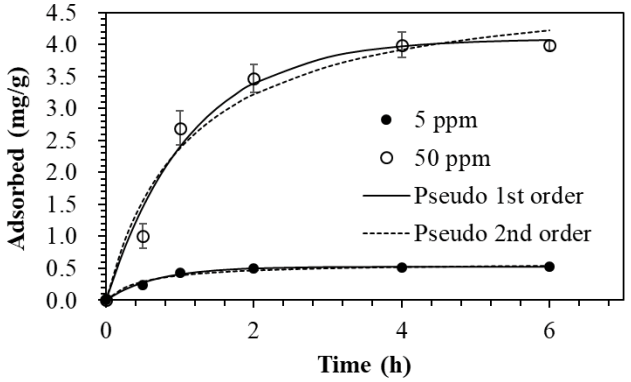


Fig. 5. Experimental kinetic adsorption data and model fits for triclosan adsorption by RH-300 at two different initial triclosan concentrations (initial triclosan concentrations: 5 and 50 mg/L, pH: 5.6, adsorbent dosage: 0.2 g, reaction time: 0–6 h, agitation speed: 100 rpm, and temperature: 25°C).

been preferred to estimate the monomolecular adsorption capacity, $Q_m$, that completes monolayer coverage on the adsorbent surface [40].

$K_L$, which is related to the energy of adsorption between the adsorbent and the adsorbate [41], was 0.037 L/mg for RH-300. The $K_L$ of RH-300 was lower than that of commercial powdered activated carbon (1.0 L/mg) [17] and similar to that of multi-walled carbon nanotubes (0.03 L/mg) [42]. The 1/$n$ value for the Freundlich model was 0.556 for RH-300, which is higher than 0.5, indicating that the binding between triclosan and RH-300 was not strong [43]. The maximum adsorption capacity ($Q_m$) of RH-300 for triclosan was comparable to that of other previously reported adsorbents. The maximum triclosan adsorption capacity of RH-300 was 72.7 mg/g. This is much larger than the adsorption capacity of clay minerals such as kaolinite and montmorillonite [17] and is similar to those of charcoal-based activated carbon (67.1 mg/g) [17] and commercial powdered activated carbon (76.3 mg/g) [30].

### 3.5. Adsorption thermodynamic parameters

Thermodynamic parameters, including the change in enthalpy ($\Delta H°$), entropy ($\Delta S°$), and free energy ($\Delta G°$), for the adsorption of triclosan onto RH-300 were quantified using Eqs. (5)–(8) and presented in Table 4. Enthalpy ($\Delta H°$) for triclosan adsorption was positive, suggesting that the adsorption of triclosan by RH-300 was an endothermic process. The enthalpy change ($\Delta H°$) was high at 42.8 kJ/mol, indicating that complexation or chemisorption may be responsible for triclosan adsorption onto RH-300. The enthalpy change in chemical adsorption was >29 kJ/mol, and that in complexation ranged from 8 to 60 kJ/mol [44,45]. Entropy ($\Delta S°$) was also positive (Table 4), indicating that there was an increase in randomness at the solid–liquid interface during the adsorption of triclosan

Table 3
Equilibrium model parameters obtained from model fitting of the experimental data for the adsorption of triclosan to RH-300

| Model | Parameters | | $R^2$ |
|---|---|---|---|
| Langmuir | $Q_m$ (mg/g) 72.7 | $K_L$ (L/mg) 0.037 | 0.952 |
| Freundlich | $K_F$ ((mg/g)·(L/mg)$^{1/n}$) 5.1 | 1/$n$ 0.556 | 0.913 |

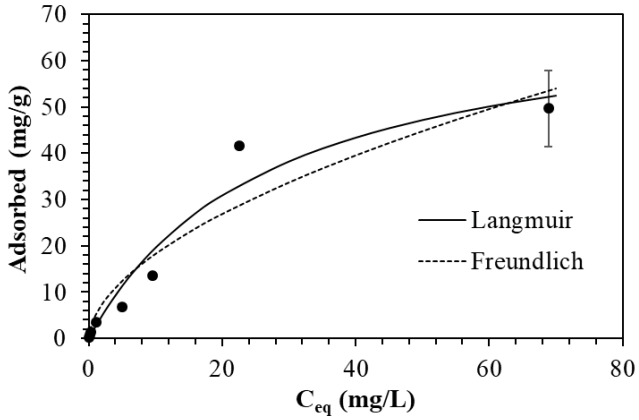


Fig. 6. Equilibrium adsorption experimental data and model fits for triclosan adsorption by RH-300 (initial triclosan concentration: 0–400 mg/L, pH: 5.6, adsorbent dosage: 0.2 g, reaction time: 6 h, agitation speed: 100 rpm, and temperature: 25°C).

Table 4
Thermodynamic parameters for the adsorption of triclosan on RH-300

| Temperature (K) | $\Delta H°$ (kJ/mol) | $\Delta S°$ (kJ/mol K) | $\Delta G°$ (kJ/mol) |
|---|---|---|---|
| 288.15 | 42.8 | 0.162 | –2.58 |
| 298.15 | | | –4.19 |
| 308.15 | | | –5.81 |

onto RH-300. The randomness at the solid–liquid interface could have resulted from the higher translational entropy acquired by the displaced water molecules as compared to that loss as a result of triclosan uptake [46]. Free energy ($\Delta G^\circ$) values obtained were negative (Table 4). Higher negative values of free energy ($\Delta G^\circ$) were obtained at higher temperatures, suggesting that the adsorption process at higher temperatures was more spontaneous.

### 3.6. Effect of pH on the adsorption of triclosan

The effect of pH was investigated by varying the pH from 4.0 to 10.0 at two different adsorbent dosages (3.33 and 6.67 g/L). The original pH of the triclosan solution was 5.6, which was adjusted by using either HCl or NaOH. Fig. 7 shows that changing the pH values over the range of 4–10 affected the adsorption of triclosan on RH-300. It was observed that the adsorbed amount of triclosan ranged from 6.4 to 6.2 mg/g in the pH values of 4–10 at 6.67 g/L of adsorbent dosage, indicating that the influence of pH on triclosan adsorption was not distinct under high dosages of the adsorbent. At the 3.33 g/L adsorbent dosage, the adsorbed amount of triclosan ranged from 11.1 to 10.9 mg/g between pH 4 and 8. When the pH increased from 8 to 10, the adsorbed amount of triclosan decreased sharply from 10.9 to 7.0 mg/g. The adsorption capacity of triclosan is dependent on not only pH, but also adsorbent dosage. At a higher dosage (6.67 g/L), the difference in the triclosan adsorption amount as a function of pH was not significant due to the sufficient amount of adsorption sites to remove 50 mg/L triclosan. However, the insufficient amount of adsorption sites at the lower dosage resulted in the triclosan adsorption depending on pH.

A similar trend was also reported in a previous study by Behera et al. [17]. At acidic pH, the total charge on the activated carbon surface was positive and triclosan ($pK_a$ = 8.14) was mainly undissociated, which caused minimum electrostatic repulsive interactions and enhanced adsorption [17]. Moreover, under highly acidic conditions (lower pH), the adsorbent surface became more positively charged and reduced the attraction between the adsorbent and the adsorbate [47]. At higher pH values, the electrostatic repulsion between the deprotonated triclosan and the negatively charged activated carbon surface reduced triclosan removal and its adsorption capacity [17].

### 3.7. Effect of fulvic acid on adsorption

To investigate the influence of natural organic matter as a competitor of triclosan, triclosan adsorption on RH-300 was assessed in the presence of different concentrations of fulvic acid, a main fraction of dissolved organic matter with high solubility [48]. The triclosan adsorption on RH-300 in the presence of fulvic acid concentrations from 0 to 100 mg/L is presented in Fig. 8. The adsorption amount of triclosan in the presence of 10 mg/L fulvic acid was 25.3% less than that in the absence of fulvic acid, indicating that the presence of fulvic acid in solution inhibited the adsorption of triclosan onto RH-300. This phenomenon can be attributed to two reasons. First, fulvic acid may compete with triclosan for favorable adsorption sites of RH-300.

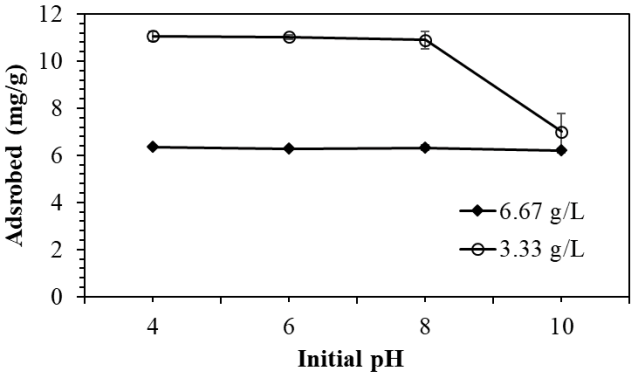


Fig. 7. Effects of solution pH on triclosan adsorption on RH-300 at two different dosing amounts (3.33 and 6.67 g/L) of RH-300 (initial triclosan concentration: 50 mg/L, pH: 5.6, adsorbent dosage: 0.1 and 0.2 g, reaction time: 6 h, agitation speed: 100 rpm, and temperature: 25°C).

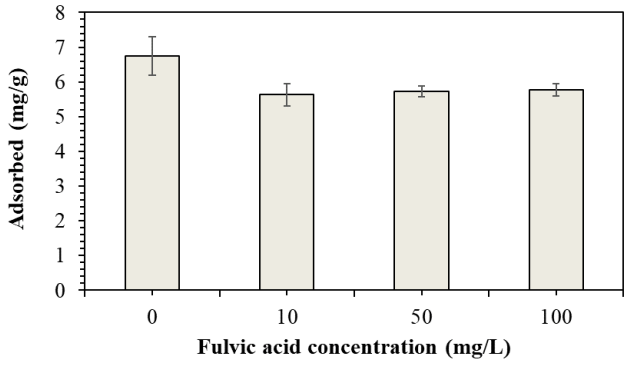


Fig. 8. Effects of fulvic acid concentration (0–100 mg/L) on triclosan adsorption by RH-300 (initial triclosan concentration: 50 mg/L; pH: 5.6; adsorbent dosage: 0.2 g; reaction time: 6 h; agitation speed: 100 rpm; temperature: 25°C).

Another reason is that large molecules of fulvic acid were adsorbed on the entrance of the pores of RH-300, blocking access of triclosan to adsorption sites within the pores [37]. As fulvic acid concentration increased from 10 to 100 mg/L, the change in triclosan adsorption was not distinct. These results indicate that triclosan adsorption onto RH-300 is stronger than that of fulvic acid [37]. The triclosan more strongly adsorbed onto the RH-300 than fulvic acid did, due to its high hydrophobicity and low electrostatic repulsion. Triclosan has greater hydrophobicity than fulvic acid. At pH 6, fulvic acid possesses negative charges, while the triclosan molecule is not deprotonated because its $pK_a$ is 8.14 as described above. Consequently, the adsorption of triclosan will be more favorable than that of fulvic acid due to lower electrostatic repulsion between the organic molecules and the surface of the RH-300.

## 4. Conclusion

In this study, the removal of triclosan from aqueous solution using rice husks thermally treated at different

temperatures was investigated. Rice husks thermally treated at 300°C showed the highest triclosan removal due to their larger pore size compared to the other rice husks. The pseudo-first-order model well described the kinetic experimental data, indicating that diffusion is a rate limiting factor for triclosan adsorption on RH-300. The Langmuir model was more suitable for describing triclosan adsorption than the Freundlich model was, indicating that triclosan was adsorbed onto RH-300 via monolayer adsorption. The adsorption of triclosan onto RH-300 is an endothermic and spontaneous reaction. The adsorption of triclosan at different pH levels was also dependent on the dosage of RH-300 and the change in triclosan adsorption was more distinct at smaller dosages. The presence of fulvic acid inhibited the adsorption of triclosan onto RH-300 but its effectiveness above 10 mg/L was constant. This study demonstrates that RH-300 can be considered an effective adsorbent for triclosan removal from wastewater because of its low cost and high adsorption capacity.

## Acknowledgments

This work was supported by the Korea Institute of Planning and Evaluation for Technology in Food, Agriculture, Forestry, and Fisheries (IPET) through the Animal Disease Management Technology Development Program, and funded by the Ministry of Agriculture, Food, and Rural Affairs (MAFRA) (Grant No. 118095-2).

## References

[1] F. Tohidi, Z. Cai, Fate and mass balance of triclosan and its degradation products: comparison of three different types of wastewater treatments and aerobic/anaerobic sludge digestion, J. Hazard. Mater., 323(Pt A) (2017) 329–340.
[2] G.-G. Ying, X.-Y. Yu, R.S. Kookana, Biological degradation of triclocarban and triclosan in a soil under aerobic and anaerobic conditions and comparison with environmental fate modelling, Environ. Pollut., 150 (2007) 300–305.
[3] G.-G. Ying, R.S. Kookana, Triclosan in wastewaters and biosolids from Australian wastewater treatment plants, Environ. Int., 33 (2007) 199–205.
[4] L. Xin, Y. Sun, J. Feng, J. Wang, D. He, Degradation of triclosan in aqueous solution by dielectric barrier discharge plasma combined with activated carbon fibers, Chemosphere, 144 (2016) 855–863.
[5] X. Hu, Z. Cheng, Z. Sun, H. Zhu, Adsorption of diclofenac and triclosan in aqueous solution by purified multi-walled carbon nanotubes, Pol. J. Environ. Stud., 26 (2017) 87–95.
[6] J. López-Morales, O. Perales-Pérez, F. Román-Velázquez, Sorption of triclosan onto tyre crumb rubber, Adsorpt. Sci. Technol., 30 (2012) 831–845.
[7] A.B. Dann, A. Hontela, Triclosan: environmental exposure, toxicity and mechanisms of action, J. Appl. Toxicol., 31 (2011) 285–311.
[8] S. Liu, R. Xu, Adsorption characteristics of triclosan on chitosan/poly(vinyl alcohol) composite nanofibrous membranes, Appl. Mech. Mater., 448–453 (2014) 134–138.
[9] J.C. Carlson, M.I. Stefan, J.M. Parnis, C.D. Metcalfe, Direct UV photolysis of selected pharmaceuticals, personal care products and endocrine disruptors in aqueous solution, Water Res., 84 (2015) 350–361.
[10] C. Zhao, H. Xie, J. Xu, X. Xu, J. Zhang, Z. Hu, C. Liu, S. Liang, Q. Wang, J. Wang, Bacterial community variation and microbial mechanism of triclosan (TCS) removal by constructed wetlands with different types of plants, Sci. Total Environ., 505 (2015) 633–639.
[11] R. Xu, Y. Si, X. Wu, F. Li, B. Zhang, Triclosan removal by laccase immobilized on mesoporous nanofibers: strong adsorption and efficient degradation, Chem. Eng. J., 255 (2014) 63–70.
[12] S. Wang, X. Wang, K. Poon, Y. Wang, S. Li, H. Liu, S. Lin, Z. Cai, Removal and reductive dechlorination of triclosan by *Chlorella pyrenoidosa*, Chemosphere, 92 (2013) 1498–1505.
[13] B. Ertit Taştan, G. Dönmez, Biodegradation of pesticide triclosan by A. versicolor in simulated wastewater and semi-synthetic media, Pestic. Biochem. Physiol., 118 (2015) 33–37.
[14] Y.-Z. Ren, M. Franke, F. Anschuetz, B. Ondruschka, A. Ignaszak, P. Braeutigam, Sonoelectrochemical degradation of triclosan in water, Ultrason. Sonochem., 21 (2014) 2020–2025.
[15] J. Chen, R. Qu, X. Pan, Z. Wang, Oxidative degradation of triclosan by potassium permanganate: kinetics, degradation products, reaction mechanism, and toxicity evaluation, Water Res., 103 (2016) 215–223.
[16] N.K.E. Mohd Khori, T. Hadibarata, M.S. Elshikh, A. Ahmed Al-Ghamdi, S. Salmiati, Z. Yusop, Triclosan removal by adsorption using activated carbon derived from waste biomass: isotherms and kinetic studies, J. Chin. Chem. Soc., 65 (2018) 951–959.
[17] S.K. Behera, S.-Y. Oh, H.-S. Park, Sorption of triclosan onto activated carbon, kaolinite and montmorillonite: effects of pH, ionic strength, and humic acid, J. Hazard. Mater., 179 (2010) 684–691.
[18] N.A. Rahmat, A.A. Ali, Salmiati, N. Hussain, M.S. Muhamad, R.A. Kristanti, T. Hadibarata, Removal of Remazol brilliant blue R from aqueous solution by adsorption using pineapple leaf powder and lime peel powder, Water Air Soil Pollut., 227 (2016) 105.
[19] I.A.W. Tan, A.L. Ahmad, B.H. Hameed, Enhancement of basic dye adsorption uptake from aqueous solutions using chemically modified oil palm shell activated carbon, Colloids Surf., A, 318 (2008) 88–96.
[20] T.S.Y. Choong, T.N. Wong, T.G. Chuah, A. Idris, Film-pore-concentration-dependent surface diffusion model for the adsorption of dye onto palm kernel shell activated carbon, J. Colloid Interface Sci., 301 (2006) 436–440.
[21] A.R. Hidayu, N. Muda, Preparation and characterization of impregnated activated carbon from palm kernel shell and coconut shell for $CO_2$ capture, Procedia Eng., 148 (2016) 106–113.
[22] M. Ahmaruzzaman, V.K. Gupta, Rice husk and its ash as low-cost adsorbents in water and wastewater treatment, Ind. Eng. Chem. Res., 50 (2011) 13589–13613.
[23] Y. Zhou, L. Zhang, Z. Cheng, Removal of organic pollutants from aqueous solution using agricultural wastes: a review, J. Mol. Liq., 212 (2015) 739–762.
[24] S. Yi, B. Gao, Y. Sun, J. Wu, X. Shi, B. Wu, X. Hu, Removal of levofloxacin from aqueous solution using rice-husk and wood-chip biochars, Chemosphere, 150 (2016) 694–701.
[25] E.A. Abigail M., R. Chidambaram, Rice husk as a low cost nanosorbent for 2,4-dichlorophenoxyacetic acid removal from aqueous solutions, Ecol. Eng., 92 (2016) 97–105.
[26] L. Shi, X. Zho, S. Zhou, Z. Yalei, Adsorption Isotherm and Thermodynamic of Triclosan on Activated Sludge, 2011 International Conference on Electric Technology and Civil Engineering, Lushan, China, 2011, pp. 975–978.
[27] A.A. Sharipova, S.B. Aidarova, N.E. Bekturganova, A. Tleuova, M. Schenderlein, O. Lygina, S. Lyubchik, R. Miller, Triclosan as model system for the adsorption on recycled adsorbent materials, Colloids Surf., A, 505 (2016) 193–196.
[28] S.B. Daffalla, H. Mukhtar, M.S. Shaharun, Characterization of adsorbent developed from rice husk: effect of surface functional group on phenol adsorption, J. Appl. Sci., 10 (2010) 1060–1067.
[29] M.C. Hoyos-Sánchez, A.C. Córdoba-Pacheco, L.F. Rodríguez-Herrera, R. Uribe-Kaffure, Removal of Cd(II) from aqueous media by adsorption onto chemically and thermally treated rice husk, J. Chem., 2017 (2017) 1–8.
[30] H. Kaur, A. Bansiwal, G. Hippargi, G.R. Pophali, Effect of hydrophobicity of pharmaceuticals and personal care products for adsorption on activated carbon: adsorption isotherms, kinetics and mechanism, Environ. Sci. Pollut. Res., 25 (2018) 20473–20485.

[31] R. Baccar, M. Sarrà, J. Bouzid, M. Feki, P. Blánquez, Removal of pharmaceutical compounds by activated carbon prepared from agricultural by-product, Chem. Eng. J., 211–212 (2012) 310–317.
[32] W.W. Simons, The Sadtler Handbook of Infrared Spectra, S.R. Laboratories, Sadtler, 1978.
[33] J. Tang, H. Lv, Y. Gong, Y. Huang, Preparation and characterization of a novel graphene/biochar composite for aqueous phenanthrene and mercury removal, Bioresour. Technol., 196 (2015) 355–363.
[34] J. Coates, Interpretation of Infrared Spectra, A Practical Approach, R.A. Meyers, Ed., Encyclopedia of Analytical Chemistry, John Wiley & Sons, Chichester, 2006, pp. 1–23.
[35] S. Abrishamkesh, M. Gorji, H. Asadi, G. Bagheri-Marandi, A. Pourbabaee, Effects of rice husk biochar application on the properties of alkaline soil and lentil growth, Plant Soil Environ., 61 (2015) 475–482.
[36] D. Lin, B. Xing, Adsorption of phenolic compounds by carbon nanotubes: role of aromaticity and substitution of hydroxyl groups, Environ. Sci. Technol., 42 (2008) 7254–7259.
[37] H.-H. Cho, H. Huang, K. Schwab, Effects of solution chemistry on the adsorption of ibuprofen and triclosan onto carbon nanotubes, Langmuir, 27 (2011) 12960–12967.
[38] Y. Liu, X. Zhu, F. Qian, S. Zhang, J. Chen, Magnetic activated carbon prepared from rice straw-derived hydrochar for triclosan removal, RSC Adv., 4 (2014) 63620–63626.
[39] Y.S. Ho, G. McKay, Pseudo-second order model for sorption processes, Process Biochem., 34 (1999) 451–465.
[40] A. Ergene, K. Ada, S. Tan, H. Katırcıoğlu, Removal of Remazol Brilliant Blue R dye from aqueous solutions by adsorption onto immobilized *Scenedesmus quadricauda*: equilibrium and kinetic modeling studies, Desalination, 249 (2009) 1308–1314.
[41] X. Guo, F. Chen, Removal of arsenic by bead cellulose loaded with iron oxyhydroxide from groundwater, Environ. Sci. Technol., 39 (2005) 6808–6818.
[42] S. Zhou, Y. Shao, N. Gao, J. Deng, C. Tan, Equilibrium, kinetic, and thermodynamic studies on the adsorption of triclosan onto multi-walled carbon nanotubes, Clean Soil Air Water, 41 (2013) 539–547.
[43] American Water Works Association, J.K. Edzwald, Water Quality & Treatment: A Handbook on Drinking Water, 6th ed., McGraw-Hill Education, New York, NY, 2011.
[44] D. Duranoğlu, A.W. Trochimczuk, U. Beker, Kinetics and thermodynamics of hexavalent chromium adsorption onto activated carbon derived from acrylonitrile-divinylbenzene copolymer, Chem. Eng. J., 187 (2012) 193–202.
[45] D.P. Mungasavalli, T. Viraraghavan, Y.-C. Jin, Biosorption of chromium from aqueous solutions by pretreated *Aspergillus niger*: batch and column studies, Colloids Surf., A, 301 (2007) 214–223.
[46] A.A. Inyinbor, F.A. Adekola, G.A. Olatunji, Kinetics, isotherms and thermodynamic modeling of liquid phase adsorption of Rhodamine B dye onto *Raphia hookerie* fruit epicarp, Water Resour. Ind., 15 (2016) 14–27.
[47] M.M.S. Saif, N.S. Kumar, M.N.V. Prasad, Binding of cadmium to *Strychnos potatorum* seed proteins in aqueous solution: adsorption kinetics and relevance to water purification, Colloids Surf., B, 94 (2012) 73–79.
[48] H. Gao, J. Chen, Y. Zhang, X. Zhou, Sulfate radicals induced degradation of triclosan in thermally activated persulfate system, Chem. Eng. J., 306 (2016) 522–530.